Modeling Thermal Conductivity of Electrolyte Mixtures in Wide Temperature and Pressure Ranges: Seawater and Its Main Components

P. Wang & A. Anderko

International Journal of Thermophysics
Journal of Thermophysical Properties and Thermophysics and Its Applications

ISSN 0195-928X
Volume 33
Number 2

Int J Thermophys (2012) 33:235-258
DOI 10.1007/s10765-012-1154-8

Springer

Int J Thermophys (2012) 33:235–258
DOI 10.1007/s10765-012-1154-8

Modeling Thermal Conductivity of Electrolyte Mixtures in Wide Temperature and Pressure Ranges: Seawater and Its Main Components

P. Wang · A. Anderko

Received: 1 September 2011 / Accepted: 6 January 2012 / Published online: 24 January 2012

Abstract A model has been established for calculating the thermal conductivity of aqueous electrolyte solutions containing the Na^+, K^+, Mg^{2+}, Ca^{2+}, Cl^-, $SO_4{}^{2-}$, $CO_3{}^{2-}$, $HCO_3{}^-$, and Br^- ions. The model is based on a previously developed computational framework for the thermal conductivity of mixed-solvent electrolyte systems, which has been expanded by explicitly accounting for pressure effects in addition to temperature and electrolyte composition effects. The model consists of a contribution of the solvent, a contribution of individual species expressed using modified Riedel coefficients, and an ionic strength-dependent term that is due to interactions between species. The model accurately represents the thermal conductivity of solutions containing single and multiple salts at temperatures ranging from 273 K to 573 K, pressures up to at least 1400 bar, and concentrations up to the limit of solid saturation. Further, the model has been applied to seawater and used to elucidate the discrepancies between the experimental data for seawater and those for Na–K–Mg–Ca–Cl–SO_4 salt solutions. With parameters evaluated on the basis of data for binary and multicomponent salt solutions, the model provides reliable predictions of the thermal conductivity of seawater.

Keywords Electrolytes · Salt solutions · Seawater · Thermal conductivity

1 Introduction

The thermal conductivity of aqueous electrolyte solutions is of great practical significance for a variety of applications in the chemical process industries, desalination, absorption refrigeration, power generation, geothermal systems, and ocean energy utilization. In the past three decades, a large number of experimental studies have been devoted to the elucidation of the effects of temperature, pressure, and electrolyte

P. Wang · A. Anderko (✉)
OLI Systems Inc., 108 American Rd., Morris Plains, NJ 07950, USA
e-mail: aanderko@olisystems.com

composition on the thermal conductivity of binary and multicomponent salt solutions [1–12]. Thus, an extensive database exists that makes it possible to develop a comprehensive model for thermal conductivity.

In a previous study [13], a model was developed for calculating the thermal conductivity of aqueous, non-aqueous, and mixed-solvent electrolyte systems ranging from dilute solutions to fused salts or pure solutes. This model expanded the concepts that were originally introduced by Riedel [14], who identified universal contributions of individual ions to the thermal conductivity of electrolyte solutions. Based on this foundation, the model incorporated the effects of interactions between species and expressed them as functions of ionic strength and temperature. This approach was shown to be valid for concentrated solutions in wide ranges of temperature. However, the resulting model was designed strictly for applications in the chemical process industry, in which there is no need to account for the effect of high pressures. Thus, its applicability was limited to pressure ranges that do not significantly exceed the vapor–liquid saturation pressure.

In this study, we focus on electrolyte systems that are important in natural environments. Such systems contain primarily the Na^+, K^+, Mg^{2+}, Ca^{2+}, Cl^-, $SO_4{}^{2-}$, $CO_3{}^{2-}$, and $HCO_3{}^-$ ions in various concentrations. Of particular interest is the thermal conductivity of seawater in wide ranges of salinity, temperature, and pressure. In the past two decades, significant progress has been reported in the development of comprehensive equations of state for predicting the Gibbs energy and all derivative properties of seawater [15–17]. This work resulted in a release of the International Association for the Properties of Water Steam [18], which provides a recommended formulation for predicting the thermodynamic properties of seawater. It is thus of considerable practical interest to establish methods for predicting transport properties of seawater, which would supplement the already available thermodynamic formulation.

The previously developed model for mixed-solvent electrolyte solutions [13] provides a suitable foundation for reproducing the behavior of Na–K–Mg–Ca–Cl–SO_4–CO_3–HCO_3–Br–H_2O systems and, in particular, of seawater. However, it is necessary to augment this model by explicitly accounting for the pressure effects. Such effects are of particular practical interest for seawater applications. Thus, the objective of this study is threefold:

(1) Extend the electrolyte solution thermal conductivity model [13] to include pressure effects, thus creating a model that is capable of reproducing thermal conductivity in wide ranges of electrolyte concentration, temperature, and pressure,
(2) Develop a comprehensive set of model parameters for Na–K–Mg–Ca–Cl–SO_4–CO_3–HCO_3–Br–H_2O systems on the basis of experimental data for systems containing single and multiple salts, and
(3) Apply the model to predict the thermal conductivity of seawater in a wide range of conditions and verify it on the basis of available data.

2 Thermal-Conductivity Model

In a previous paper [13], a general framework was derived for representing the thermal conductivity of electrolyte systems in mixed solvents. Here, we summarize this framework in a form that is appropriate for solutions in a single solvent, i.e., water.

The thermal conductivity of an electrolyte solution is expressed as a sum of three contributions, i.e.,

$$\lambda = \lambda_{H_2O} + \Delta\lambda^{s} + \Delta\lambda^{s-s} \tag{1}$$

where λ_{H_2O} is the thermal conductivity of the solvent (water), $\Delta\lambda^{s}$ is a contribution of individual species, and $\Delta\lambda^{s-s}$ is a contribution of interactions between pairs of species. For aqueous systems, the λ^0 term is calculated from the 2011 IAPWS formulation for the thermal conductivity of pure water [19] and is evaluated at the temperature and pressure of the mixture.

The $\Delta\lambda^{s}$ term is characterized by ion-specific coefficients and can be interpreted as the result of ion-solvent interactions. It constitutes a generalization of Riedel's additivity rule for ions [14], in which mole fractions rather than molar concentrations are used as composition variables:

$$\Delta\lambda^{s} = \sum_i x_i \alpha_i \tag{2}$$

where the subscript i pertains to all solutes (ions and ion pairs), x_i is the mole fraction, and α_i is the mole fraction-based Riedel coefficient of the ith species. The temperature dependence of the α_i coefficient is given by

$$\alpha = \alpha_1 + \alpha_2 \exp\left[-K(T - T_0)\right] \tag{3}$$

where T is the temperature in K, $T_0 = 273.15$ K, and K is a universal constant equal to 0.023 as established in the previous paper [13]. The coefficients α_1 and α_2 are determined on the basis of experimental data for binary systems at low or moderate electrolyte concentrations. The concentration range that is appropriate for the determination of the α_i parameters is determined as the range over which the concentration dependence of thermal conductivity is nearly linear and, therefore, the $\Delta\lambda^{s}$ term is dominant. Within the concentration region in which the $\Delta\lambda^{s}$ term is predominant, the coefficients can be evaluated using the simple formula, $\lambda - \lambda_{H_2O} = x_c\alpha_c + x_a\alpha_a$ [13]. Following Riedel [14], the α coefficient for the Na^+ ion is assigned a value of zero at all temperatures, i.e., $\alpha_{Na^+} = 0$, thus establishing a reference for other ions. With this assumption, coefficients for all other ions can be determined. If ion pairs are present in a solution, the α_i parameter of an ion pair is calculated as a sum of the α_i parameters for the constituent ions. Therefore, the $\Delta\lambda^{s}$ term is the same whether or not ion pairs exist in a solution.

The species–species interaction term is expressed as

$$\Delta\lambda^{s-s} = \sum_i \sum_k f_i f_k \beta_{ik} \tag{4}$$

where the indices i and k pertain to all solutes, β_{ik} is a binary parameter, and f_i and f_k are solute-only mole fractions of the ith and kth species, adjusted for the charges of the species, i.e.,

$$f_i = \frac{x_i / \max(1, |z_i|)}{\sum_m x_m / \max(1, |z_m|)} \tag{5}$$

and the index m pertains to all solute species. In its most general form, the binary parameter β_{ik} is expressed as a function of ionic strength as

$$\beta_{ik} = \beta_{ik}^{(1)} + \beta_{ik}^{(2)} I_x^2 + \beta_{ik}^{(3)} \exp\left(\beta_{ik}^{0} I_x\right) \tag{6}$$

The parameter I_x in Eq. 6 is an extended ionic strength that accounts for the presence of neutral ion pairs (as opposed to solvent molecules). Such ion pairs may become significant for some salts at high concentrations because of speciation equilibria.

$$I_x = \frac{1}{2} \sum_{\text{ions}} z_i^2 x_i + \sum_{\text{ion-pair}} x_n \tag{7}$$

At low and moderate pressures, e.g., near vapor–liquid saturation, the temperature dependence of the three $\beta_{ik}^{(m)}$ $(m = 1, 2, 3)$ parameters is given by

$$\beta_{ik}^{(m)} = \beta_{ik}^{(m0)} \exp\left[\beta_{ik}^{(mT)} (T - T_0)\right] \tag{8}$$

where $\beta_{ik}^{(m0)}$ and $\beta_{ik}^{(mT)}$ are adjustable parameters.

2.1 Pressure Dependence

In this study, we introduce an additional pressure dependence in order to reproduce thermal conductivity in wide ranges of both temperature and pressure. Experimental data indicate a nearly linear pressure dependence of the thermal conductivity of electrolyte solutions up to at least 1400 bar. This is illustrated in Fig. 1 for aqueous NaCl solutions. In view of the model (Eq. 1), this behavior is partially accounted for by the pressure dependence of pure water thermal conductivity and partially by that of the solute-dependent terms. Since the contribution of individual species, $\Delta\lambda^{s}$, is primarily responsible for the effects of low electrolyte concentrations at which the pressure dependence is dominated by that of the solvent, there is no need to introduce a pressure dependence explicitly into $\Delta\lambda^{s}$. On the other hand, the species interaction contribution $\Delta\lambda^{s-s}$ requires an explicit pressure dependence because it determines the effect of electrolytes at high concentrations. Considering the near-linear pressure dependence of the thermal conductivity of electrolyte solutions and that of pure water at corresponding temperatures and pressures, Eq. 8 needs to be extended by adding a term that is linear with respect to pressure. Accordingly, the interaction parameters $\beta_{ik}^{(m)}(m = 1, 2, 3)$ are rewritten to include both temperature and pressure effects, i.e.,

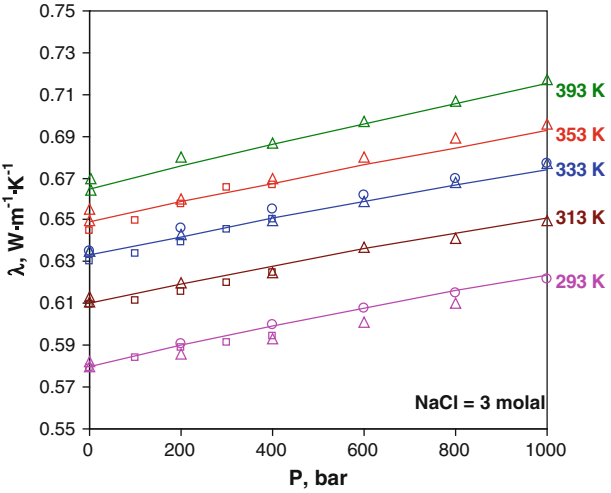

Fig. 1 Calculated and experimental pressure dependence of thermal conductivity of 3 molal NaCl solutions at various temperatures. The experimental data are from Magomedov [1] (*circles*), Abdulagatov and Magomedov [2] (*triangles*), and Nagasaka et al. [10] (*squares*)

$$\beta_{ik}^{(m)} = \beta_{ik}^{(m0)} \exp\left[\beta_{ik}^{(mT)}(T - T_0)\right] + \beta_{ik}^{(mP)}(P - P_0), \tag{9}$$

where $P_0 = 1$ bar and $\beta_{ik}^{(m0)}$, $\beta_{ik}^{(mT)}$, and $\beta_{ik}^{(mP)}$ are adjustable constants.

The parameters $\beta_{ik}^{(m0)}$, $\beta_{ik}^{(mT)}$, and $\beta_{ik}^{(mP)}$ are determined by regressing experimental data for concentrated electrolyte systems. For most solutions, only a relatively small subset of the possible parameters is regressed, depending on the range of available experimental data.

3 Determination of Parameters

The model has been applied to aqueous systems containing the Na^+, K^+, Mg^{2+}, Ca^{2+}, Cl^-, $SO_4{}^{2-}$, $HCO_3{}^-$, $CO_3{}^{2-}$, and Br^- ions. A substantial amount of experimental data is available for these systems in the literature. In particular, comprehensive measurements have been reported for binary and multicomponent mixtures of NaCl, KCl, $MgCl_2$, $CaCl_2$, Na_2SO_4, K_2SO_4, and $MgSO_4$ over wide ranges of composition, temperature, and pressure [1–12]. For other salts, data are available at moderate pressures, near vapor–liquid saturation. Table 1 summarizes the literature sources that were used in the development of model parameters.

Before applying the model to reproduce the experimental data, it is worthwhile to examine the uncertainty of the data and, by extension, the expected reasonable level of deviations between the data and calculated results. Since the IAPWS formulation for pure water [19] is used here as a foundation for the model for electrolyte solutions, the estimated uncertainty of the thermal conductivity of pure water should serve as a baseline for the expected uncertainty for mixtures. According to the IAPWS release

Table 1 Summary of sources of experimental data for binary and multicomponent systems that were used to establish the parameters of the model

System	References
Binary systems	
$NaCl + H_2O$	Nagasaka et al. [10], Magomedov [1], Abdulagatov and Magomedov [2], Abdullayev et al. [7], Ramires et al. [11], Assael et al. [5], Riedel [14], Kapustinskii and Ruzavin [20], Vargaftik and Osminin [21], Davis et al. [22], Yusufova et al. [23], El'darov [6]
$KCl + H_2O$	Abdulagatov and Magomedov [2], Magomedov [1], Assael et al. [5], Ramires et al. [12], Riedel [14], Kapustinskii and Ruzavin [20], Vargaftik and Osminin [21], Davis et al. [22]
$MgCl_2 + H_2O$	Kapustinskii and Ruzavin [20], Chernen'kaya and Vernigora [24], Riedel [14], Rau [25], Aseyev [26]
$CaCl_2 + H_2O$	Assael et al. [5], Kapustinskii and Ruzavin [20], Riedel [14], Meyer [27], Rau [25], Chernen'kaya and Vernigora [24], Aseyev [26]
$Na_2SO_4 + H_2O$	Kapustinskii and Ruzavin [20], Riedel [14], Aseyev [26]
$K_2SO_4 + H_2O$	Abdulagatov and Azizov [4], Riedel [14], Aseyev [26]
$MgSO_4 + H_2O$	Riedel [14], Aseyev [26]
$Na_2CO_3 + H_2O$	Riedel [14], Aseyev [26], Chernen'kaya and Vernigora [24]
$NaHCO_3 + H_2O$	Aseyev [26], Chernen'kaya and Vernigora [24]
$K_2CO_3 + H_2O$	Riedel [14], Aseyev [26]
$KHCO_3 + H_2O$	Aseyev [26]
$NaBr + H_2O$	Aseyev [26]
Multicomponent systems	
$NaCl + KCl + H_2O$	Magomedov [3]
$NaCl + CaCl_2 + H_2O$	Abdullayev et al. [7]
$NaCl + Na_2SO_4 + H_2O$	Magomedov [3]
$MgCl_2 + MgSO_4 + H_2O$	Magomedov [3]
$NaCl + MgCl_2 + CaCl_2 + H_2O$	Magomedov [3]
$NaCl + KCl + CaCl_2 + H_2O$	El'darov [8,9]

[19], the estimated uncertainty of pure water thermal conductivity is 0.7 % along the saturation line and rises to 1.5 % for temperatures up to ~523 K and pressures up to 50 MPa. This range encompasses the majority of the data that are used here. For pressures between 50 MPa and 250 MPa and temperatures up to 700 K, which cover the remainder of the electrolyte solution database, the estimated uncertainty is 2 %. Thus, the overall expected uncertainty of thermal conductivity of electrolyte solutions should not be better than these estimates. This is in agreement with the available estimates of uncertainty for electrolyte solutions. For the data sets that are limited to temperatures up to about 373 K and pressures along the saturation line, the uncertainty has been reported to be better than 0.5 % [5,11,12]. This level of uncertainty can be also confirmed by comparing data from various sources (Table 1) within this range of temperature and pressure. For the data sets that extend to high temperatures (up to

Table 2 Individual aqueous species considered in this study and parameters for calculating their contributions to thermal conductivity (Eq. 3)

Species	α_{1,H_2O}	α_{2,H_2O}	Molality in reference seawater [39]
Na^+	0.0	0.0	0.4860597
Mg^{2+}	−0.496250	0.052652	0.0547421
Ca^{2+}	−0.052799	0.126519	0.0106568
K^+	−0.382485	0.044932	0.0105797
Cl^-	−0.360439	0.006076	0.5657647
$SO_4{}^{2-}$	−0.029457	0.044903	0.0292643
$HCO_3{}^-$	−0.215690	−0.167037	0.0017803
Br^-	−1.147163	0.249998	0.0008728
$CO_3{}^{2-}$	0.341711	0.0	0.0002477

573 K) and pressures (up to 140 MPa), the uncertainty is estimated to be, in general, less than 2 % [1–4]. Thus, the model is expected to reproduce the experimental data within these uncertainties.

In the first step of parameter regressions, the coefficients α_1 and α_2 have been determined for individual ions based on experimental data in fairly dilute binary solutions [13]. These parameters are collected in Table 2. Since the α_1 and α_2 parameters pertain to individual ions, they remain valid for all binary and multicomponent solutions. In the second step, the parameters $\beta_{ik}^{(m0)}$, $\beta_{ik}^{(mT)}$, and $\beta_{ik}^{(mP)}$ have been determined for all cation–anion combinations on the basis of data for concentrated binary systems. In the final step, data for systems containing two or more salts were analyzed to evaluate the relevant cation–cation and anion–anion parameters. It should be noted that parameters between like ions constitute a second-order correction compared with those between unlike ions. Nevertheless, they are significant to obtain optimum accuracy. The data that are available for seawater were not used in the regression of parameters, and the experimental database was limited to the systems listed in Table 1. The consequences of this choice will be analyzed further in Sect. 4.

The obtained values of the parameters $\beta_{ik}^{(m0)}$, $\beta_{ik}^{(mT)}$, and $\beta_{ik}^{(mP)}$ are summarized in Table 3. The parameter matrix is fairly sparse, as the selection of parameters is guided primarily by the complexity of the concentration dependence of thermal conductivity. In particular, the $\beta_{ik}^{(30)}$ and $\beta_{ik}^{(0)}$ parameters have been found necessary for only three pairs of ions, and the $\beta_{ik}^{(3T)}$ and $\beta_{ik}^{(3P)}$ parameters were never used. The pressure-dependent thermal-conductivity parameters that have been obtained in this work replace the parameters that were developed in the previous, pressure-independent version of the model [13]. However, the pressure-independent parameters that are available for other species pairs remain valid over a narrow pressure range and can be used for mixture calculations together with the parameters listed in Table 3.

The numerical values of the parameters of the thermal-conductivity model depend on the speciation of the system. Although the individual species contribution $\Delta\lambda^s$ does not depend on ion pairing, $\Delta\lambda^{s-s}$ is influenced by the presence of ion pairs.

Table 3 Binary ion–ion parameters in the thermal conductivity model

Ion pair		$\beta^{(10)}$	$\beta^{(20)}$	$\beta^{(30)}$	$\beta^{(0)}$	$\beta^{(1T)}$	$\beta^{(2T)}$	$\beta^{(1P)}$	$\beta^{(2P)}$
Ca^{2+}	Na^+	0.393279	53.6907			−0.0127655	0.0032884	-5.7153×10^{-5}	−0.131628
Cl^-	$SO_4{}^{2-}$	−0.476331	7.39369	0.64766	−6.7955	0.0011964	0.0022777		
K^+	Ca^{2+}		0.140609				0.032807		1.71576
K^+	Cl^-		−0.109253				0.024143		−0.0181361
K^+	Na^+		28.4987				0.0045518		
K^+	$SO_4{}^{2-}$		−4.88329				0.0085209		−0.0060100
Mg^{2+}	Ca^{2+}	0.000757	−113.373			0.0330266	0.0022158	0.0149972	−1.71478
Mg^{2+}	Cl^-	0.0344483	−0.797660	−0.0374002	0.820409	−0.0204675	−0.0906346		0.00799346
Mg^{2+}	Na^+	0.392105	28.5040			−0.104770	−0.00152455	−0.00123718	0.245534
Mg^{2+}	$SO_4{}^{2-}$		−0.879678				0.00777823		−0.0416195
Na^+	Br^-	0.008051							
Na^+	Cl^-	0.00348241	−3.00155			0.00718169	−0.00069711	-4.3196×10^{-6}	−0.0083663
Na^+	$CO_3{}^{2-}$	−0.12133	−19.0519	0.104008	9.82429	−0.00160097	−0.0042375		
Na^+	$HCO_3{}^{2-}$		−77.1356						

In this study, the computation of thermal conductivity was preceded by the calculation of speciation for all conditions of temperature, pressure, and composition. Then, the obtained mole fractions of ions and ion pairs were used in Eqs. 1–9. If speciation was neglected, the species–species interaction parameters would be somewhat different from the values listed in Table 3. For speciation calculations, a previously developed thermodynamic model [28–30] has been used. This model is summarized in the Appendix. Further, a complete set of the thermodynamic model parameters is collected in Tables 4 and 5 for Na–K–Mg–Ca–Cl–SO_4–HCO_3–CO_3–Br–H_2O systems. In the thermodynamic model, the formation of the $MgCl_{2(aq)}$, $CaCl_{2(aq)}$, $MgSO_{4(aq)}$, $CaSO_{4(aq)}$, $MgCO_{3(aq)}$, and $CaCO_{3(aq)}$ ion pairs is assumed. The concentration of these ion pairs increases, in general, as the temperature and the relevant salts' concentration are increased. For thermal-conductivity calculations over wide temperature and composition ranges, it is necessary to take into account the formation of ion pairs and to calculate their concentrations as described in the Appendix. However, for calculations in a more limited space of temperature and solution composition, it is possible to neglect the formation of ion pairs and assume that the concentrations of all ions are equal to their nominal (or analytical) values. The errors introduced by the neglect of ion pairing will be discussed further in Sect. 4.

4 Results and Discussion

4.1 Single-Salt Solutions

With the parameters listed in Tables 2 and 3, the model represents the thermal conductivity of single-salt solutions essentially within experimental uncertainty. This is illustrated in Figs. 1 and 2 for NaCl + H_2O and in Fig. 3 for KCl + H_2O. As shown in Fig. 1, the pressure dependence of the thermal conductivity of NaCl + H_2O solutions at fixed concentrations and temperatures is nearly linear, at least up to 1000 bar. Figure 2 shows the temperature dependence of thermal conductivity for a fixed NaCl concentration at pressures varying from vapor–liquid saturation (1 bar to 20 bar depending on temperature) up to 1000 bar. The λ versus T curves show maxima at temperatures ranging from ~410 K to 430 K, depending on the pressure. An increase in pressure shifts the λ versus T curves towards higher conductivities, in agreement with the pressure dependence illustrated in Fig. 1. At the same time, the maxima become less pronounced at higher pressures, which is due to a stronger pressure effect at higher temperatures. The experimental data for the NaCl + H_2O solutions that are summarized in Table 1 are, in general, in reasonably good agreement with each other. The model reproduces the data of Nagasaka et al. [10], Assael et al. [5], Magomedov [1], Abdulagatov and Magomedov [2], Ramires et al. [11], and Abdullayev et al. [7] with an average deviation of 0.50 % over a temperature range from 274.1 K to 473.15 K, at pressures from 1 bar to 1000 bar and for NaCl mole fractions ranging from 0 to 0.096 (or molalities up to 5.89). This concentration range is reasonably close to the solubility limit of NaCl.

Figure 3 illustrates the temperature dependence of the thermal conductivity of KCl + H_2O solutions for various compositions ranging from 2.5 wt% to 25 wt% KCl.

Table 4 Parameters used in the thermodynamic model for individual ionic and neutral species: standard partial molar Gibbs energy of formation, entropy, and parameters of the Helgeson–Kirkham–Flowers equation of state [42–46] for standard partial molar thermodynamic properties ($a_{HKF,1,...,4}$,$c_{HKF,1}$, $c_{HKF,2}$, ω)

Species	$\Delta\overline{G}^0_f$ (kJ · mol^{-1})	$\overline{S}^0$(J · mol^{-1} · K^{-1})	$a_{HKF,1}$	$a_{HKF,2}$	$a_{HKF,2}$	$a_{HKF,3}$	$c_{HKF,1}$	$c_{HKF,2}$	ω
Na^{+a}	−261.881	58.4086	0.1839	−228.5	3.256	−27260	18.18	−29810	33060
K^{+a}	−282.462	101.044	0.3559	−147.3	5.435	−27120	7.4	−17910	19270
Mg^{2+a}	−453.960	−138.100	−0.08217	−859.9	8.39	−23900	20.8	−58920	153720
Ca^{2+a}	−552.790	−56.484	−0.01947	−725.2	5.2966	−24792	9	−25220	123660
Cl^{-a}	−131.290	56.735	0.4032	480.1	5.563	−28470	−4.4	−57140	145600
$SO_4{}^{2-a}$	−744.495	18.828	0.83014	−198.46	−6.2122	−26970	1.64	−179980	314630
Br^{-a}	−104.053	82.8432	0.5269	659.4	4.745	−31430	−3.8	−68110	138580
$MgCl_{2(ab)}{}^b$	−623.223	2.8920	0.62187	740.58	2.8322	−30851	23.961	32720	−3800
$CaCl_{2(ab)}{}^b$	−794.040	67.7344	0.62187	740.58	2.8322	−30851	23.961	32720	−3800
$MgSO_{4(ab)}{}^b$	−1192.380	10.6358	0	0	0	0	0	0	0
$CaSO_{4(ab)}{}^b$	−1311.00	27.5149	0.24079	−189.92	6.4895	−27004	−8.4942	−81271	−100
$MgCO_{3(ab)}{}^b$	−1004.34	57.4894	−0.07355	−957.45	9.5062	−23831	−10.2416	−86159	−3800
$CaCO_{3(ab)}{}^b$	−1099.61	41.2383	−0.03907	−873.25	9.1753	−24179	−11.5309	−90641	−3800

[a] Parameters were obtained from [46–50]

[b] Parameters of the ion pairs were adjusted in this study based on multiproperty regressions for binary salt-water systems [28,52]

Table 5 Binary parameters used in the ionic interaction term (Eqs. A6–A7)

Species$i$	Species j	$b_{0,ij}$	$b_{1,ij}$	$b_{2,ij}$	$b_{3,ij}$	$b_{4,ij}$	$c_{0,ij}$	$c_{1,ij}$	$c_{2,ij}$	$c_{3,ij}$	$c_{4,ij}$
Na^+	Cl^-	15611	7.9642	−357990	−0.0036431	−2892.7	−30086	−15.010	699850	0.0068210	5552.3
Na^+	$SO_4{}^{2-}$	54889	25.452	−1320670	−0.010792	−10024	−99000	−45.463	2.4044	0.019281	18048
Na^+	$HCO_3{}^-$	115.42	−0.16614	−19956	0	0	−223.57	0.33162	39807	0	0
Na^+	$CO_3{}^{2-}$	−185.30	0.77147	4695.4	−0.0009064	0	141.71	−0.97790	19526	0.0014692	0
K^+	Cl^-	15088	7.2361	−354190	−0.0031415	−2771.6	−26853	−12.857	635046	0.0056499	4927.6
K^+	$SO_4{}^{2-}$	242.38	−0.33309	−50023	0	0	−491.11	0.71822	99893	0	0
K^+	$HCO_3{}^-$	−65.408	0.093347	10980	0	0	0	0	2380.9	0	0
K^+	$CO_3{}^{2-}$	103.87	−0.12725	−29244	0	0	−322.26	0.46417	71799	0	0
Mg^{2+}	Cl^-	−46.090	0.036682	−12896	8.2938×10^{-6}	0	110.43	−0.24025	11645	0.00031976	0
Mg^{2+}	$SO_4{}^{2-}$	−179.74	0.27012	14930	0	0	86.576	0	8980.2	0	0
Mg^{2+}	$HCO_3{}^-$	0	0	2479.1	0	0	0	0	0	0	0
Ca^{2+}	Cl^-	−95.993	0.47023	−17371	-5.6755×10^{-4}	0	−0.69437	−0.42158	43726	0.00079111	0
Ca^{2+}	$SO_4{}^{2-}$	10888	−16.973	−1770400	0	0	−15416	24.216	2508590	0	0
Ca^{2+}	$HCO_3{}^-$	−287.82	0.51115	48333	0	0	0	0	0	0	0
Ca^{2+}	$CO_3{}^{2-}$	0	0	−155596	0	0	0	0	265383	0	0
Na^+	K^+	−93.0411	−0.234488	37002.7	5.62879×10^{-4}	0	−64.633	0.881525	−29428.5	−0.0012859	0
Na^+	Mg^{2+}	−28.8624	0.0351923	8744.27	0	0	0	0	−6373.88	0	0

Table 5 continued

Species i	Species j	$b_{0,ij}$	$b_{1,ij}$	$b_{2,ij}$	$b_{3,ij}$	$b_{4,ij}$	$c_{0,ij}$	$c_{1,ij}$	$c_{2,ij}$	$c_{3,ij}$	$c_{4,ij}$
Na^+	Ca^{2+}	11.2685	−0.026379	2905.5	0	0	0	0	−6685.21	0	0
K^+	Mg^{2+}	−28.2506	0.0311345	16139.0	0	0	0	0	−13262.6	0	0
K^+	Ca^{2+}	−43.804	0.0468862	23092.5	0	0	0	0	−18687.4	0	0
Cl^-	$SO_4{}^{2-}$	−7.1362	0.010742	1712.4	0	0	0	0	0	0	0
Cl^-	$HCO_3{}^-$	−4.5121	0.010091	0	0	0	0	0	0	0	0
Cl^-	$CO_3{}^{2-}$	0.84118	0	504.19	0	0	0	0	0	0	0
$SO_4{}^{2-}$	$CO_3{}^{2-}$	41.194	−0.034779	0	0	0	−50.512	0	0	0	0
$CaCl_{2(aq)}$	Na^+	−27.3022	0	17433.	0	0	0	0	0	0	0
$CaCl_{2(aq)}$	K^+	−24.2268	0	18665.2	0	0	0	0	0	0	0
$CaCl_{2(aq)}$	H_2O	−9.09197	0	0	0	0	0	0	0	0	0
$MgCl_{2(aq)}$	Na^+	0	0	−11710.7	0	0	0	0	0	0	0
$MgCl_{2(aq)}$	K^+	0	0	−9228.3	0	0	0	0	0	0	0
$MgSO_{4(aq)}$	Cl^-	0	0	−1669.9	0	0	0	0	0	0	0
$CaSO_{4(aq)}$	Na^+	−194.69	0.33604	28460	0	0	0	0	0	0	0
$CaSO_{4(aq)}$	K^+	372.48	−0.34581	−86359	0	0	0	0	0	0	0
$CaSO_{4(aq)}$	Mg^{2+}	0	0	−10443	0	0	0	0	0	0	0
$CaSO_{4(aq)}$	Cl^-	205.01	−0.27042	−41233	0	0	0	0	0	0	0
$CaCO_{3(aq)}$	Na^+	0	0	2791.9	0	0	0	0	0	0	0
$CaCO_{3(aq)}$	K^+	0	0	2791.9	0	0	0	0	0	0	0

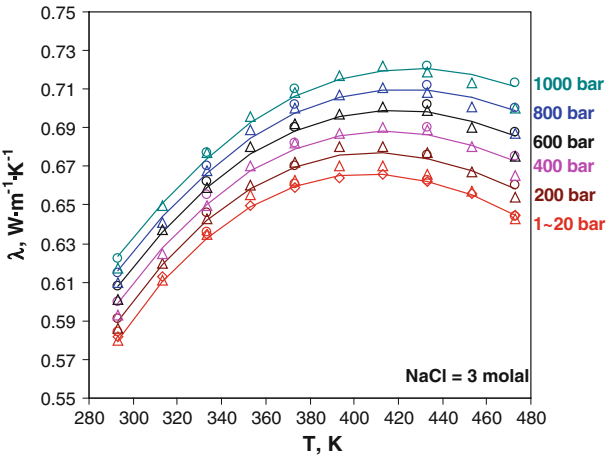

Fig. 2 Calculated and experimental temperature dependence of thermal conductivity of 3 molal NaCl solutions at various pressures. The experimental data are from Magomedov [1] (*circles*), Abdulagatov and Magomedov [2] (*triangles*), and Abdullayev et al. [7] (*diamonds*)

The figure shows two families of λ versus T curves—one for pressures near vapor–liquid saturation and one for 400 bar. In a characteristic pattern, the λ versus T curves for various compositions are nearly parallel and shift towards lower λ values as the KCl concentration increases. An increase in pressure shifts the curves towards higher conductivity values and somewhat flattens the maximum with respect to temperature, as already observed for NaCl solutions. The average deviation between the model calculations and the experimental data of Assael et al. [5], Magomedov [1], Abdulagatov and Magomedov [2], and Ramires et al. [12] is 0.47 % for temperatures ranging from 293.15 K to 473.15 K, pressures up to 1 000 bar, and KCl mole fractions up to 0.0745 (or molalities up to 4.47).

The thermal conductivity of other binary systems (cf., Table 1) is reproduced by the model with a similar accuracy. Also, the qualitative patterns that are shown in Figs. 1, 2, and 3 remain valid for all salt solutions that are examined in this study.

4.2 Solutions of Multiple Salts

The experimental results of Magomedov [3], Abdullayev et al. [7], and El'darov [8,9] provide an extensive database for multicomponent Na–K–Mg–Ca–Cl–SO_4 systems. They make it possible to verify and calibrate the model for various combinations of salts over wide ranges of temperature, pressure, and composition. Examples of calculations for multicomponent systems are shown in Figs. 4 and 5.

Figure 4 compares the calculated and experimental thermal conductivities in the $NaCl + MgCl_2 + CaCl_2 + H_2O$ system. The upper and lower diagrams in Fig. 4 show the temperature dependence of λ for various fixed solution compositions in the vicinity of the saturation pressure and at 400 bar, respectively. It is noteworthy that the λ versus T curves have the same shape as those for single-salt solutions (cf., Fig. 3).

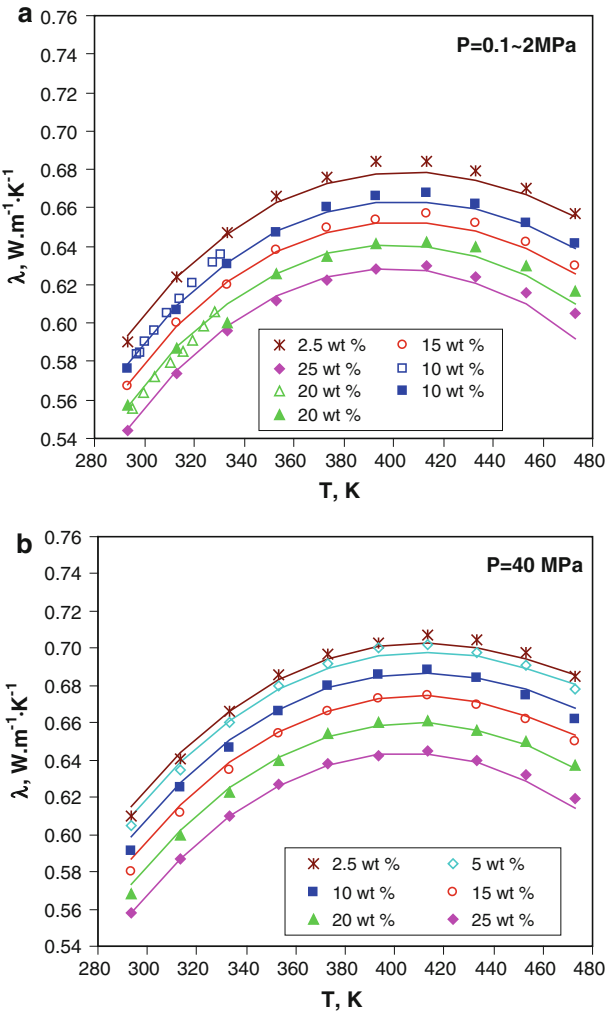

Fig. 3 Calculated and experimental thermal conductivity of KCl–H_2O solutions as a function of temperature for various KCl concentrations at pressures (a) near vapor–liquid saturation and (b) 40 MPa. The experimental data are from Assael et al. [5] (*hollow squares* and *triangles* at temperatures up to ~330 K) and Abdulagatov and Magomedov [2] (*remaining symbols*)

Accordingly, as the overall salt content of the solution increases, the λ versus T curves shift towards lower values, whereas an increase in pressure raises the value of λ, especially at higher temperatures. Also, the λ versus T curves for various salt contents are nearly parallel. The average deviation between the calculated values and the data of Magomedov [3] is 0.30 % for temperatures ranging from 293.15 K to 573.25 K, pressures up to 400 bar, and various salt contents. This deviation is similar, but slightly lower than that obtained for single-salt solutions over comparable ranges of conditions. This is due primarily to the fact that only one literature source was used for

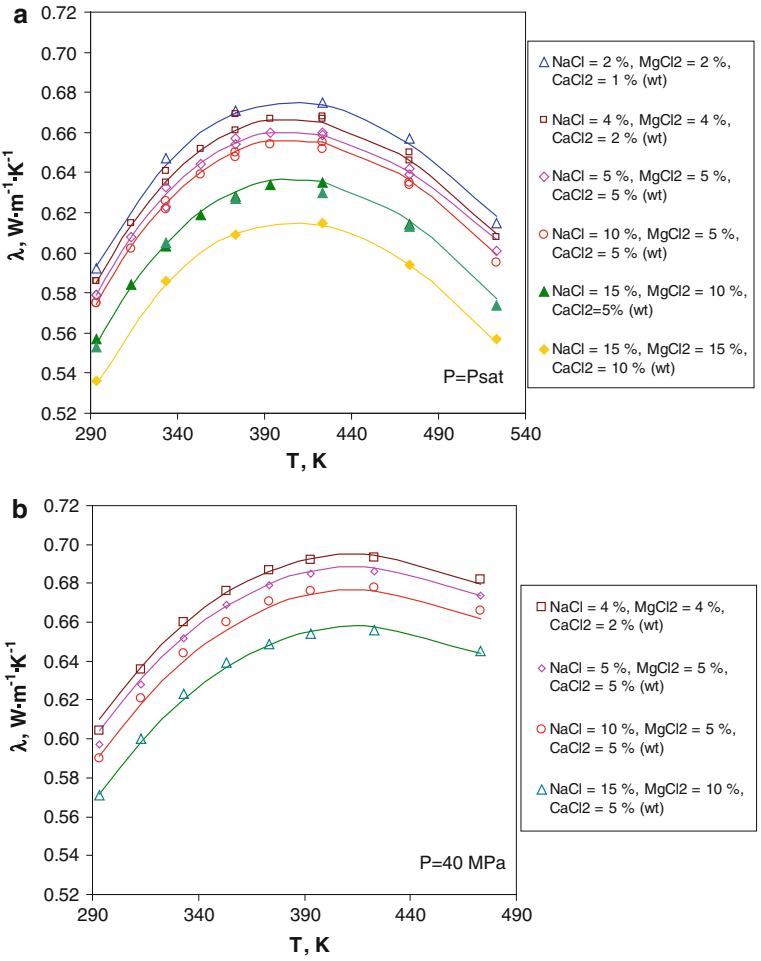

Fig. 4 Calculated and experimental thermal conductivity of the NaCl–$MgCl_2$–$CaCl_2$–H_2O solution as a function of temperature for various salt concentrations (a) near vapor–liquid saturation pressure and (b) at 40 MPa. The experimental data are from Magomedov [3]

the $NaCl + MgCl_2 + CaCl_2 + H_2O$ system, whereas multiple data sets were used for single-salt solutions such as $NaCl + H_2O$ and $KCl + H_2O$. Thus, the relatively minor discrepancies between various data sources resulted in the slightly higher deviations for single-salt systems compared to those for the $NaCl + MgCl_2 + CaCl_2 + H_2O$ system.

Figure 5 shows the behavior of the $NaCl + KCl + CaCl_2 + H_2O$ multicomponent system. The upper diagram combines the λ versus T curves for various total salt compositions at a fixed ratio of individual salts, whereas the lower diagram shows the λ versus T curves at a fixed total composition at various pressures. It is interesting to note that the pressure effect is more pronounced than the salt concentration effect, in particular, at higher temperatures. The model reproduces the experimental data of

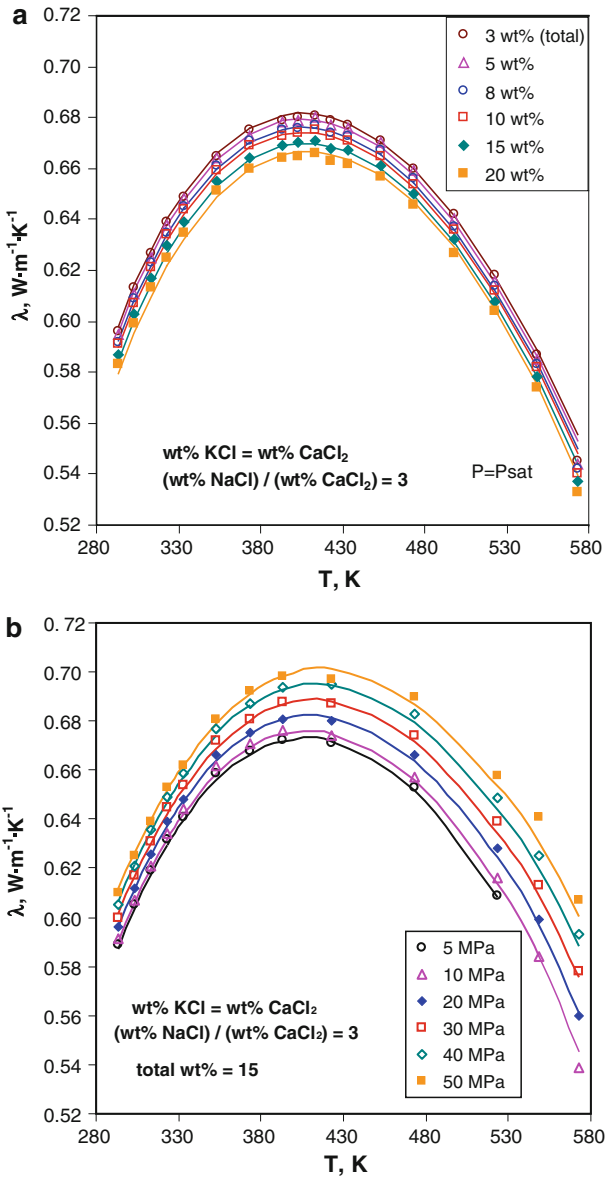

Fig. 5 Calculated and experimental thermal conductivity of the NaCl–KCl–$CaCl_2$–H_2O system as a function of temperature for (a) various salt concentrations at vapor–liquid saturation and (b) various pressures at a fixed salt concentration of 15 wt%. The experimental data are from El'darov [8,9]

El'darov [8,9] with an average deviation of 0.30 % over a temperature range from 293.15 K to 573.22 K and a pressure range from vapor–liquid saturation to 500 bar. The remaining multicomponent systems (cf., Table 1) are reproduced with a similar accuracy.

4.3 Seawater

The results that have been obtained for various Na–K– Mg–Ca–Cl–SO_4 systems (cf., Table 1; Figs. 1, 2, 3, 4, 5) indicate that there is a high degree of consistency between the binary and multicomponent systems over wide ranges of temperature, pressure, and composition. Therefore, the experimental data listed in Table 1 made it possible to evaluate the model parameters with a high level of confidence. However, the thermal conductivity data that are available for seawater show a considerably lower level of mutual consistency. Therefore, we have not made any attempt to make adjustments of model parameters on the basis of seawater data. Instead, we retain the parameters that were determined on the basis of the experimental data listed in Table 1, and we predict the thermal conductivity of seawater.

The species that are listed in Table 2 cover the most important constituents of seawater. For all of these species, the model parameters reported in Tables 2 and 3 are firmly grounded in experimental data. The Na^+, K^+, Mg^{2+}, Ca^{2+}, Cl^-, and ${SO_4}^{2-}$ ions, for which we have both binary and multicomponent data, are by far the most abundant ionic constituents of seawater. Also, the HCO_3^-, ${CO_3}^{2-}$, and Br^- ions have been included. While only binary data are available for the sodium and potassium salts of these ions, their concentrations in seawater are so low that their effect is accounted for practically only by their single-species contributions (cf., Table 2). The remaining species (i.e., Sr^{2+}, ${B(OH)_4}^-$, $B(OH)_3$, F^-, OH^-, and CO_2) have very low concentrations in seawater, and their contribution to bulk properties such as thermal conductivity is negligible.

Experimental data for the thermal conductivity of seawater have been recently reviewed by Sharqawy et al. [31,32]. The data are available from multiple sources [33–38] and span a reasonably wide range of pressures (up to 1400 bar), temperatures (from 273.15 K to 453.15 K), and salinities (up to 153.46 $g \cdot kg^{-1}$). For the calculation of the thermal conductivity of seawater, the reference seawater composition [39] was used. For completeness, the reference concentrations are listed in Table 2 for the species that were included in the calculations. In order to apply the model to seawater and to compare the results with experimental data, the reported salinities have been recalculated into concentrations of the constituent species by maintaining the concentration ratios in reference seawater (cf., the last column in Table 2).

Figures 6, 7, and 8 compare the predictions of the present model with the experimental data. Figure 6 shows the pressure dependence of the thermal conductivity of seawater with salinities of 31.5 $g \cdot kg^{-1}$ and 35 $g \cdot kg^{-1}$ at temperatures ranging from 273.15 K to 333.15 K. As with NaCl solutions (cf., Fig. 1), the thermal conductivity nearly linearly increases with pressure up to 1400 bar. The agreement with the experimental data of Caldwell [33] is excellent. The average deviation is only 0.33 %, which is remarkable considering that Caldwell's data [33] were not used in the regression of the model parameters. This deviation is essentially identical to the stated uncertainty of Caldwell's [33] measurements, which is estimated at 0.3 % by the author. On the other hand, the data of Castelli et al. [34] are systematically shifted towards lower values of λ compared with the Caldwell [33] data (cf., Fig. 6). Therefore, the average deviation from the data of Castelli et al. [34] is 2.10 %, which is more than six times higher than the deviation from the data of Caldwell [33]. Although Castelli et al. [34]

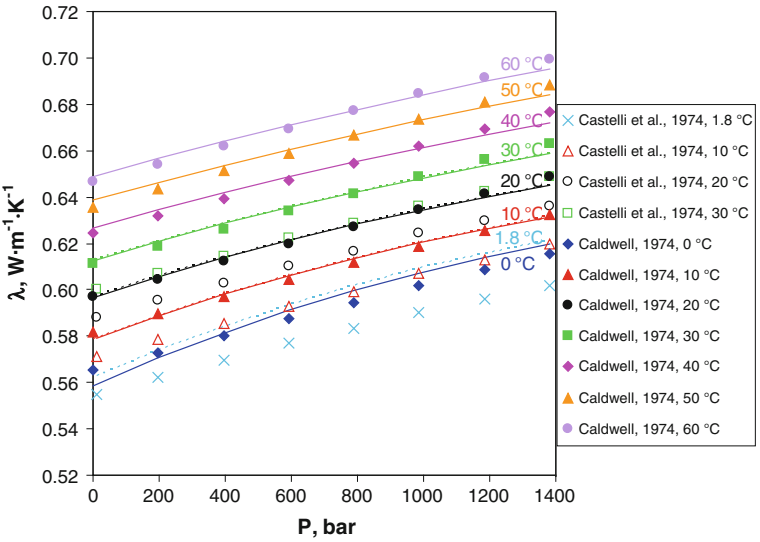

Fig. 6 Comparison of calculated thermal conductivities of seawater (*lines*) with experimental data of Castelli et al. [34] (*hollow symbols*) and Caldwell [33] (*solid symbols*). The *solid* and *dotted lines* have been calculated for salinities of 31.5 $g \cdot kg^{-1}$ and 35 $g \cdot kg^{-1}$, respectively. The *lines* are labeled with the temperatures for which they were generated

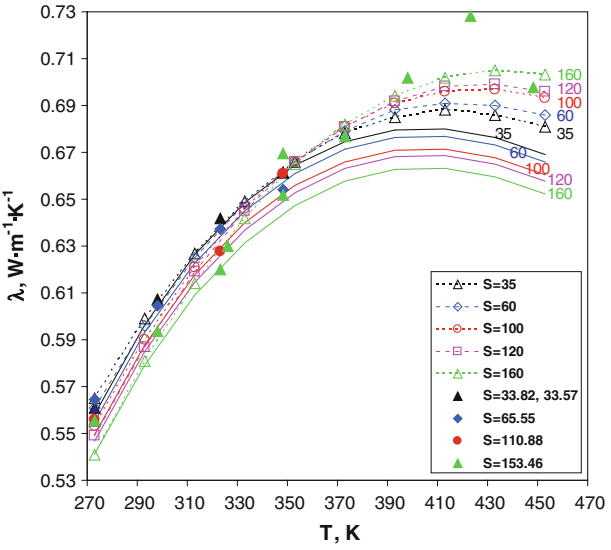

Fig. 7 Comparison of thermal conductivities of seawater calculated from the present model (*solid lines*) with Jamieson and Tudhope's [35] raw experimental data (*solid symbols*) and smoothed values (*hollow symbols connected with dotted lines* as a guide to the eye). The *solid* and *dotted lines* are labeled with the values of salinity (in $g \cdot kg^{-1}$) for which they were generated

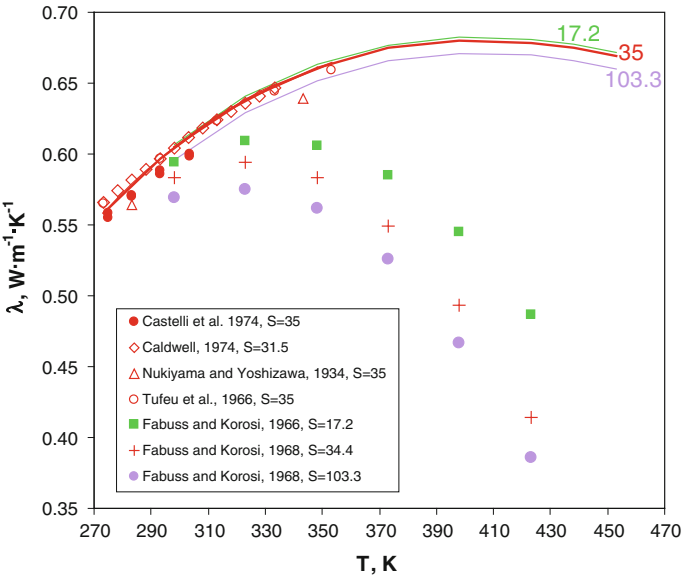

Fig. 8 Comparison of seawater thermal conductivities calculated from the present model (*lines*) with the experimental data of Castelli et al. [34], Caldwell [33], Nukiyama and Yoshizawa [37], Tufeu et al. [36], and Fabuss and Korosi [38]. The *lines* are labeled with the values of salinity (in $g \cdot kg^{-1}$) for which they were generated

estimate the uncertainty of their measurements at 1.06 %, the deviations between their data and those of Caldwell [33] are higher and are 2 %.

Figure 7 compares the predictions with the data of Jamieson and Tudhope [35], which, unlike the other seawater data, cover a rather wide range of salinity and temperature. Jamieson and Tudhope [35] reported a matrix of experimental data for salinities from 33.57 $g \cdot kg^{-1}$ to 153.46 $g \cdot kg^{-1}$ in the temperature range from 273.15 K to 348.15 K and an additional series of measurements for salinities of 153.46 $g \cdot kg^{-1}$ up to 448.15 K. Based on these data, they developed a set of smoothed values, which are shown in Fig. 7 as hollow symbols connected by dotted lines. The predicted thermal conductivities are in very good agreement with the data of Jamieson and Tudhope [35] up to ~323.15 K. Beyond this temperature, increasing deviations are observed. It is noteworthy that the smoothed data of Jamieson and Tudhope [35] show a crossover at ~360 K. Below the crossover temperature, the thermal conductivities decrease with salinity, whereas they are reported to show the opposite trend above this temperature (cf., Fig. 7, dotted lines). Such a crossover is not supported by any other experimental data for Na–K–Mg–Ca–Cl–SO_4 systems and should be regarded as an artifact of Jamieson and Tudhope's [35] smoothing procedure. Thus, the hollow symbols in Fig. 7 cannot be regarded as reliable estimates of thermal conductivity at high temperatures. The λ versus T curves predicted by the model are roughly parallel for various salinities, which is consistent with the behavior of various salt solutions. The overall average deviation between the predictions and the data of Jamieson and Tudhope [35] is 1.79 %, which encompasses deviations ranging from fractions of a percent at low

temperatures to more than 7 % as a maximum deviation at high temperatures. The stated experimental uncertainty of the data of Jamieson and Tudhope [35] is 3 %, which is substantially higher than the uncertainty of the data of Caldwell [33] and Castelli et al. [35] and exceeds the average deviation between the predictions and the data (i.e., 1.79 %).

Finally, Fig. 8 compares the predicted λ versus T curves near vapor–liquid saturation with the remaining seawater data that are available in the literature. The predictions are in excellent agreement with the data of Caldwell [33] and Tufeu et al. [36]. The agreement with the data of Castelli et al. [34] and Nukiyama and Yoshizawa [37] is reasonable, but the deviations are somewhat higher than the stated experimental uncertainty of these data. The data of Fabuss and Korosi [38] are in complete disagreement with all other data and with the calculations, but it should be noted that Fabuss and Korosi stated themselves that their data should be considered tentative. Considering the limitations of the currently available data, new accurate experimental measurements for seawater at high temperatures (above 350 K) would be very useful for an unequivocal verification of the predictions.

It is also of interest to estimate the error that results from neglecting the Sr^{2+}, $B(OH)_4{}^-$, $B(OH)_3$, F^-, and OH^- species. Since their concentrations in seawater are low, their effect is accounted for by the $\Delta\lambda^s$ term. By applying the revised Riedel coefficients for these species [13], it can be estimated that the seawater thermal conductivity would change by only 0.002 % if these species were included in the calculations. Such a deviation is much below the uncertainty of the most accurate measurements.

4.4 Simplified Calculations for Seawater

As described in Sect. 2, the thermal-conductivity model is mathematically simple and non-iterative. The main complexity in its implementation lies in the calculation of speciation, which needs to precede the actual computation of thermal conductivity. As described in the Appendix and the references cited therein, speciation calculations are complex and require a dedicated algorithm for solving the necessary equations. Therefore, it is of interest to examine the possibility of making simplified predictions without prior speciation calculations, i.e., by neglecting ion pairs and assuming that the actual concentrations of ions are equal to their analytical (or nominal) concentrations. In the thermodynamic model that is adopted here, NaCl and KCl are assumed not to form ion pairs at temperatures up to 300 °C. Thus, for NaCl + KCl + H_2O systems without any other ions, speciation calculations are not needed. If other ions (cf., Table 2) are included, the population of ion pairs (cf., Table 4) would increase with rising temperature and Ca, Mg, SO_4, and CO_3 content.

To estimate the effect of ion pairing on the thermal conductivity of seawater, calculations have been performed by eliminating ion pairs at high temperatures, at which the concentration of ion pairs is the highest. These calculations reveal that the error that results from neglecting ion pairing in reference-composition seawater is 0.006 % at 200 °C and rises to 0.094 % at 300 °C. If the salinity is increased to 160 $g \cdot kg^{-1}$, the corresponding errors are 0.009 % and 0.078 % at 200 °C and 300 °C, respectively. These values are well below the experimental uncertainty, even at 300 °C. Thus, it can

be concluded that the thermal conductivity of seawater can be computed with good accuracy by using Eqs. 1–9 directly without prior speciation calculations. Speciation calculations are necessary only for systems with a substantially higher Ca, Mg, SO_4, or CO_3 content than that found in seawater.

5 Conclusions

A previously developed model for calculating the thermal conductivity of electrolyte solutions has been extended by incorporating pressure effects. The revised model has been parameterized and validated for systems containing the Na^+, K^+, Mg^{2+}, Ca^{2+}, Cl^-, $SO_4{}^{2-}$, $HCO_3{}^-$, $CO_3{}^{2-}$, and Br^- ions. The thermal conductivities of both binary and multicomponent systems have been reproduced with a consistent set of parameters that reflect the contributions of individual species and species-species interactions. With optimum parameters, the obtained deviations from experimental data are comparable to experimental uncertainty. Overall, the model reproduces the thermal conductivity at temperatures ranging from 273 K to 573 K, pressures up to at least 1400 bar, and salt concentrations up to solid-liquid saturation.

Particular attention has been focused on predicting the thermal conductivity of seawater. Since the available experimental data for binary, ternary and quaternary systems from the Na–K–Mg–Ca–Cl–SO_4 family are far more comprehensive and consistent than those for seawater, the available seawater data were not used to adjust the model parameters. Instead, the model has been used to predict the thermal conductivity of seawater and to analyze the reliability of the available data. Excellent agreement has been obtained with the data of Caldwell [33] and Tufeu et al. [36] whereas the agreement with other data sources ranges from fair to poor. In general, it is believed that the model, when combined with the obtained parameters for the Na–K–Mg–Ca–Cl–SO_4–CO_3–HCO_3–Br systems, accurately predicts the thermal conductivity of seawater as well as that of its constituent salts and salt mixtures.

Acknowledgments The work reported here was supported by Alcoa, Areva, ConocoPhillips, Mitsubishi Chemical, Rohm & Haas, and Shell. The authors thank Allan H. Harvey for making available the Fortran implementation of the IAPWS Formulation 2011 for the Thermal Conductivity of Ordinary Water Substance.

Appendix: Thermodynamic Speciation Model

Thermodynamic speciation calculations have been performed using a previously developed model for multicomponent electrolyte systems [28–30]. This model, referred to as mixed-solvent electrolyte model (MSE) was described in detail in previous papers [28–30] and, therefore, this appendix gives only a brief summary.

The thermodynamic framework combines an excess Gibbs energy formulation with a treatment of speciation based on chemical equilibria. In this framework, the excess Gibbs energy is expressed as

$$\frac{G^{\mathrm{ex}}}{RT} = \frac{G^{\mathrm{ex}}_{\mathrm{LR}}}{RT} + \frac{G^{\mathrm{ex}}_{\mathrm{II}}}{RT} + \frac{G^{\mathrm{ex}}_{\mathrm{SR}}}{RT} \tag{A1}$$

where G^{ex}_{LR} represents the contribution of long-range electrostatic interactions, G^{ex}_{II} accounts for specific ionic (ion–ion and ion–molecule) interactions, and G^{ex}_{SR} is the short-range contribution resulting from intermolecular interactions.

The long-range interaction contribution is calculated from the Pitzer–Debye–Hückel formula [40] expressed in terms of mole fractions and symmetrically normalized, i.e.,

$$\frac{G^{ex}_{LR}}{RT} = -\left(\sum_i n_i\right)\frac{4A_x I_x}{\rho}\ln\left(\frac{1+\rho I_x^{1/2}}{\sum_i x_i[1+\rho\left(I^0_{x,i}\right)^{1/2}]}\right) \tag{A2}$$

where the sum is over all species, I_x is the mole fraction-based ionic strength, $I^0_{x,i}$ represents the ionic strength when the system's composition reduces to a pure component i, i.e., $I^0_{x,i} = 0.5z_i^2$; ρ is assigned, following Pitzer [40], a universal dimensionless value ($\rho = 14.0$), and A_x is given by

$$A_x = \frac{1}{3}(2\pi N_A d_s)^{1/2}\left(\frac{e^2}{4\pi\varepsilon_0\varepsilon_s k_B T}\right)^{3/2} \tag{A3}$$

where d_s and ε_s are the molar density and dielectric constant of the solvent, respectively. The specific ion–interaction contribution is calculated from an ionic strength-dependent, symmetrical second virial coefficient-type expression:

$$\frac{G^{ex}_{II}}{RT} = -\left(\sum_i n_i\right)\sum_i\sum_j x_i x_j B_{ij}(I_x) \tag{A4}$$

where $B_{ij}(I_x) = B_{ji}(I_x)$, $B_{ii} = B_{jj} = 0$, and the ionic strength dependence of B_{ij} is given by

$$B_{ij}(I_x) = b_{ij} + c_{ij}\exp(-\sqrt{I_x + a_1}) \tag{A5}$$

where b_{ij} and c_{ij} are binary interaction parameters and a_1 is set equal to 0.01. In their most general form, the parameters b_{ij} and c_{ij} are calculated as functions of temperature as

$$b_{ij} = b_{0,ij} + b_{1,ij}T + b_{2,ij}/T + b_{3,ij}T^2 + b_{4,ij}\ln T \tag{A6}$$

$$c_{ij} = c_{0,ij} + c_{1,ij}T + c_{2,ij}/T + c_{3,ij}T^2 + c_{4,ij}\ln T \tag{A7}$$

Finally, the short-range interaction contribution is calculated from the UNIQUAC equation [41]. In systems containing only strong electrolytes, such as the mixtures considered here, the short-range term is not used and all interactions are accounted for by Eq. A4.

The excess Gibbs energy model is used to calculate nonideality effects on ion pairing equilibria. For example, the formation of an ion pair $M_aX_{b(aq)}$ is represented as a

chemical equilibrium between $M_aX_{b(aq)}$ and its constituent simple ions, i.e., M^{m+} and X^{x-}. The chemical equilibrium is governed by the chemical potentials of all species that participate in a reaction. The chemical potential of each ionic or neutral species i is determined by its standard-state contribution, $\mu_i^o(T, P)$ and its activity coefficient, $\gamma_i(T, P, \boldsymbol{x})$, i.e.,

$$\mu_i(T, P, x) = \mu_i^0(T, P) + RT \ln x_i \gamma_i(T, P, x) \tag{A8}$$

The standard-state chemical potentials for aqueous species, $\mu_i^o(T, P)$, are calculated as functions of temperature and pressure using the Helgeson–Kirkham–Flowers–Tanger (HKF) equation of state [42–46]. The parameters of the HKF model are available for a large number of aqueous species including ions and ion pairs [47–51]. Since the standard-state properties calculated from the model of Helgeson et al. are based on the infinite dilution reference state and on the molality concentration scale, the activity coefficients calculated from Eq. A1 are first converted to those based on the unsymmetrical reference state, i.e., at infinite dilution in water and, second, the molality-based standard-state chemical potentials are converted to corresponding mole fraction-based quantities [28].

The parameters of the model are determined using thermodynamic data of various types (i.e., vapor–liquid equilibria, activity and osmotic coefficients, solid–liquid equilibria, enthalpies of dilution or mixing, heat capacities, and densities) as described in previous studies [28,52]. The standard-state properties of all species (i.e., ions and ion pairs) are summarized in Table 4 and the interaction parameters (Eqs. A6 and A7) are collected in Table 5. These two tables provide a complete set of parameters for speciation calculations in aqueous Na–K–Ca–Mg–Cl–SO_4–HCO_3^-–CO_3 systems.

References

1. U.B. Magomedov, High Temp. **31**, 458 (1993)
2. I.M. Abdulagatov, U.B. Magomedov, Int. J. Thermophys. **15**, 401 (1994)
3. U.B. Magomedov, High Temp. **36**, 44 (1998)
4. I.M. Abdulagatov, N.D. Azizov, Int. J. Thermophys. **26**, 593 (2005)
5. M.J. Assael, E. Charitidou, J.Ch. Stassis, W.A. Wakeham, Ber. Bunsenges. Phys. Chem. **93**, 887 (1989)
6. V.S. El'darov, Zhur. Fiz. Khim. **60**, 603 (1986)
7. K.M. Abdullayev, V.S. Eldarov, A.M. Mustafaev, High Temp. **36**, 375 (1998)
8. V.S. El'darov, High Temp. **41**(3), 327 (2003)
9. V.S. El'darov, Energetika **1**, 57 (2004)
10. Y. Nagasaka, H. Okada, J. Suzuki, A. Nagashima, Ber. Bunsenges. Phys. Chem. **87**, 859 (1983)
11. M.L.V. Ramires, C.A. Nietode de Castro, J.M.N.A. Fareleira, J. Chem. Eng. Data **39**, 186 (1994)
12. M.L.V. Ramires, C.A. Nietode de Castro, Int. J. Thermophys. **21**, 671 (2000)
13. P. Wang, A. Anderko, Ind. Eng. Chem. Res. **47**, 5698 (2008)
14. L. Riedel, Chem. Ing. Tech. **23**, 59 (1951)
15. R. Feistel, Prog. Oceanogr. **58**, 43 (2003)
16. R. Feistel, G. Marion, Prog. Oceanogr. **74**, 515 (2007)
17. R. Feistel, Deep Sea Res. **55**, 1639 (2008)
18. International Association for the Properties of Water and Steam, Release of the IAPWS Formulation for the Thermodynamic Properties of Seawater, IAPWS, Berlin, www.iapws.org
19. International Association for the Properties of Water and Steam, Release of the IAPWS Formulation 2011 for the Thermal Conductivity of Ordinary Water Substance, IAPWS, www.iapws.org

20. A.F. Kapustinskii, I.I. Ruzavin, Zhur. Fiz. Khim. **29**, 2222 (1955)
21. N.B. Vargaftik, Yu.P. Osminin, Teploenergetika **7**, 11 (1956)
22. P.S. Davis, F. Theeuwes, R.J. Bearman, R.F. Gordon, J. Chem. Phys. **55**, 4776 (1971)
23. V.D. Yusufova, R.I. Pepinov, V.A. Nikolaev, G.M. Guseinov, Inzh. Fiz. Zhur. **29**, 600 (1975)
24. E.I. Chernen'kaya, G.A. Vernigora, Zh. Prikl. Khim. **45**, 1704 (1972)
25. W. Rau, Z. Angew. Phys. **1**, 211 (1948)
26. G.G. Aseyev, *Electrolytes, Properties of Solutions, Methods for Calculation of Multicomponent Systems and Experimental Data on Thermal Conductivity and Surface Tension* (Begell House Inc., New York, 1999)
27. E. Meyer, Z. Ges. Kälte-Industrie **47**, 129 (1940)
28. P. Wang, A. Anderko, R.D. Young, Fluid Phase Equilib. **203**, 141 (2002)
29. P. Wang, R.D. Springer, A. Anderko, R.D. Young, Fluid Phase Equilib. **222–223**, 11 (2004)
30. P. Wang, A. Anderko, R.D. Springer, R.D. Young, J. Mol. Liq. **125**, 37 (2006)
31. M.H. Sharqawy, J.H. Lienhard, S.M. Zubair, Desalin. Water Treat. **16**, 354 (2010)
32. M.H. Sharqawy, J.H. Lienhard, S.M. Zubair, *Thermophysical Properties of Seawater*, http://web.mit.edu/seawater
33. D. Caldwell, Deep Sea Res. **21**, 131 (1974)
34. V. Castelli, E. Stanley, E. Fischer, Deep Sea Res. **21**, 311 (1974)
35. D.T. Jamieson, J.S. Tudhope, Desalination **8**, 393 (1970)
36. R. Tufeu, B. Le Neindre, P. Johannin, Compt. Rend. **262**, 229 (1966)
37. S. Nukiyama, Y. Yoshizawa, J. Soc. Mech. Eng. Jpn. **37**, 347 (1934)
38. B.M. Fabuss, A. Korosi, *Properties of seawater and solutions containing sodium chloride, potassium chloride, sodium sulphate and magnesium sulphate*, Office of Saline Water Research Development Progress Report No. 384, 1968
39. F.J. Millero, R. Feistel, D.G. Wright, T.J. McDougall, Deep Sea Res. I **55**, 50 (2008)
40. K.S. Pitzer, J. Am. Chem. Soc. **102**, 2902 (1980)
41. D.S. Abrams, J.M. Prausnitz, AIChE J. **21**, 116 (1975)
42. H.C. Helgeson, D.H. Kirkham, G.C. Flowers, Am. J. Sci. **274**, 1089 (1974a)
43. H.C. Helgeson, D.H. Kirkham, G.C. Flowers, Am. J. Sci. **274**, 1199 (1974b)
44. H.C. Helgeson, D.H. Kirkham, G.C. Flowers, Am. J. Sci. **276**, 97 (1976)
45. H.C. Helgeson, D.H. Kirkham, G.C. Flowers, Am. J. Sci. **281**, 1241 (1981)
46. J.C. Tanger, H.C. Helgeson, Am. J. Sci. **288**, 19 (1988)
47. E.L. Shock, H.C. Helgeson, D.A. Sverjensky, Geochim. Cosmochim. Acta **53**, 2157 (1989)
48. E.L. Shock, H.C. Helgeson, Geochim. Cosmochim. Acta **52**, 2009 (1988)
49. E.L. Shock, H.C. Helgeson, Geochim. Cosmochim. Acta **54**, 915 (1990)
50. E.L. Shock, D.C. Sassani, M. Willis, D.A. Sverjensky, Geochim. Cosmochim. Acta **61**, 907 (1997)
51. D.A. Sverjensky, E.L. Shock, H.C. Helgeson, Geochim. Cosmochim. Acta **61**, 1359 (1997)
52. M.S. Gruszkiewicz, D.A. Palmer, R.D. Springer, P. Wang, A. Anderko, J. Solut. Chem. **36**, 723 (2007)